# Secondary structure determination of $^{15}$N-labelled human Long-[Arg-3]-insulin-like growth factor 1 by multidimensional NMR spectroscopy

Leanne G. Laajoki[a], Eugene Le Breton[d], Gary K. Shooter[b], John C. Wallace[b], Geoffrey L. Francis[c], John A. Carver[d], Max A. Keniry[a,*]

[a] *Research School of Chemistry, The Australian National University, GPO Box 414, Canberra, ACT 2601, Australia*
[b] *Department of Biochemistry, University of Adelaide, Adelaide, South Australia 5000, Australia*
[c] *CSIRO Division of Human Nutrition and CRC for Tissue Growth and Repair, P.O. Box 10065, Adelaide, South Australia 5000, Australia*
[d] *Department of Chemistry, University of Wollongong, Wollongong, NSW 2522, Australia*

Received 28 October 1997

**Abstract Insulin-like growth factors (IGFs) are a group of proteins that promote cell growth and differentiation. Long-[Arg-3]-IGF-I (Francis et al. (1992) J. Mol. Endocrinol. 8, 213–223), a potent analogue of IGF-I, which has a Glu-3 to Arg-3 substitution and a hydrophobic, thirteen amino acid N-terminal extension, has been studied by $^{1}$H,$^{15}$N NMR spectroscopy. All the backbone $^{1}$H and $^{15}$N assignments and most of the $^{1}$H sidechain assignments have been completed. The secondary structure elements were identified by determining the sequential and medium range NOEs from sensitivity-enhanced $^{15}$N-NOESY-HSQC and sensitivity-enhanced $^{15}$N-HSQC-NOESY-HSQC spectra. The IGF-I domain of Long-[Arg-3]-IGF-I was found to have an almost identical structure to IGF-I. The N-terminal seven amino acid residues of the extension have very few medium range or long range NOEs but the next five amino acids form a turn-like structure that is spatially close to the beginning of helix 1 in the IGF-I domain. Hydrogen-deuterium exchange experiments show that all the slowly exchanging backbone amide protons in the IGF-I domain are either in the helical or the extended structural elements. Many of the amide protons in the N-terminal extension are also protected from the solvent although the residues in this part of the extension do not have any identifiable secondary structure. The results are interpreted in terms of the increased biological potency of Long-[Arg-3]-IGF-I and the decreased binding to insulin-like growth factor binding proteins.**



*Key words:* $^{1}$H NMR; IGF-I; Growth factor; Protein structure

## 1. Introduction

Insulin-like growth factors (IGFs) are single chain polypeptides which exhibit a high degree of sequence similarity with insulin [1–3]. The two forms, IGF-I and IGF-II, are found in plasma and most biological fluids. IGF-I is primarily known as a mitogenic agent which is involved in the regulation of cell growth and differentiation [4].

IGFs exert their biological effects by binding to target cell surface receptors and activating intracellular tyrosine kinases [5]. IGFs are often bound to insulin-like growth factor binding proteins (IGFBPs) in vivo which modulate the transport and delivery of IGFs to cell receptors [6]. The various classes of IGFBPs exhibit considerable sequence similarity among themselves. The nature of the interactions between the IGFBPs and IGFs is not known although residues on the ligand critical for binding have been identified [5,7–9].

IGF-I consists of 70 amino acids and has four well defined domains; B, C, A and D beginning from the N-terminus [4]. Fifty percent of the residues from the A and B domains are identical to the A and B domains of insulin. The C domain of IGF-I is comparable to the C domain of pro-insulin, but has no sequence homology with the latter. The D domain is a C-terminal extension of eight residues which has no corresponding segment in insulin [10]. The secondary structure [11,12] and the three-dimensional structure [12,13] of IGF-I have recently been determined by $^{1}$H NMR spectroscopy and computer-based methods. The protein contains three α-helices, the first in the B domain (Ala-8 to Cys-18), and the other two in the A domain (Ile-43 to Phe-49 and Leu-54 to Cys-61). The latter two run antiparallel to each other because of a disulphide cross-link between Cys-47 and Cys-52. The remaining two disulphide cross-links are between Cys-18 and Cys-61, and Cys-6 and Cys-48. Following α-helix 1, a β-turn leads into a poorly defined C domain. The D domain is also poorly defined.

Recombinant fusion protein analogues of IGF-I, in which the N-terminal region has been modified, show increased biological potency [7] and have attracted great commercial interest. For example, Long-[Arg-3]-IGF-I, in which Glu-3 in human IGF-I is replaced by Arg-3 and the N-terminus has a 13 amino acid extension consisting of the first 11 amino acids of methionyl porcine growth hormone followed by the dipeptide Val-Asn, is one of the most potent of these analogues [8,9]. It has been postulated that the increased potency of Long-[Arg-3]-IGF-I is due to reduced binding to the IGFBPs rather than increased affinity for the cell receptors [9]. The poor binding affinity for IGFBPs implies more free growth factor is available for interaction with the cellular receptors [9].

It is unclear whether this increased potency of Long-[Arg-3]-IGF-I is due to the N-terminal region having a direct effect on binding to IGFBPs or the N-terminal extension disrupting the secondary structure of regions of IGF-I involved in IGFBP binding. Here, we report the resonance assignment, secondary structure determination and global fold of Long-[Arg-3]-IGF-I, with particular focus on the N-terminal extension. This work serves as a basis for a future structural anal-

*Corresponding author.
E-mail: max@rsc.anu.edu.au

*Abbreviations:* HMQC, heteronuclear multiple quantum correlation; HSQC, heteronuclear single quantum correlation; IGF-I, insulin-like growth factor 1; IGF-II, insulin-like growth factor 2; IGFBPs, insulin-like growth factor binding proteins; NMR, nuclear magnetic resonance; NOESY, nuclear Overhauser effect spectroscopy; TOCSY, total correlation spectroscopy


*PII* S0014-5793(97)01496-8

ysis of the biological activity of Long-[Arg-3]-IGF-I and the design of further IGF-I analogues.

## 2. Material and methods

### 2.1. Long-[Arg-3]-IGF-I expression and purification

*E. coli* strain JM101 was transformed with the p[Met$^1$]-pGH(11)-Val-Asn-IGF-I expression vector and maintained on minimal medium as described by King et al. [8]. The Long-[Arg-3]-IGF-I expression strain was grown in a 2 l fermenter by Bresatec Ltd. (Adelaide, Australia), employing a minimal medium containing 3.22 g/l $^{15}NH_4Cl$ as the sole nitrogen source [8]. Growth was controlled at 37°C, 55% $pO_2$ and pH 7.0 maintained with NaOH feeding. Cells were induced at an optical density (OD 600) of 10 with 250 μmol/l isopropyl-β-D-thiolgalactoside and grown for a further 6 h. Homogenisation and inclusion body isolation were performed as described by King et al. [8]. $^{15}$N-labelled Long-[Arg-3]-IGF-I was refolded and purified as described by Francis et al. [9]. Amino acid analysis of the first 18 N-terminal residues was used to confirm identity and indicated >96% purity. A single species of 9222 ± 2 Da was detected by electrospray mass spectrometry, indicative of 100% incorporation of $^{15}$N (theoretical mass 9223).

### 2.2. NMR spectroscopy

NMR measurements were performed at 30°C on both $^{15}$N-labelled and unlabelled protein. The $^{15}$N-Long-[Arg-3]-IGF-I was dissolved to a concentration of 1.0 mM in 90% $H_2O$/10% $D_2O$, at pH 4.1. The unlabelled Long-[Arg-3]-IGF-I was dissolved to a concentration of 1.3 mM in 100% $D_2O$ at pH 4.1. Initial 2D and 3D NMR experiments were carried out on a Varian VXR-500S NMR spectrometer. Subsequent NMR experiments were performed on Varian INOVA-500 and Varian INOVA-600 spectrometers. The following experiments were collected on the $^{15}$N-labelled protein in 90% $H_2O$/10% $D_2O$ buffer: sensitivity-enhanced $^{15}$N-HSQC [14], $^{15}$N-HMQC-J [15], 2D $^{15}$N-HSQC-TOCSY [16] with a mixing time of 70 ms, 3D sensitivity-enhanced $^{15}$N-TOCSY-HSQC [16] with a mixing time of 70 ms, 3D sensitivity-enhanced $^{15}$N-NOESY-HSQC [16] with mixing times of 80 ms and 140 ms, 3D sensitivity-enhanced $^{15}$N-HSQC-NOESY-HSQC [16] with a mixing time of 140 ms and a 3D sensitivity-enhanced $^{15}$N-HSQC-TOCSY-NOESY-HSQC [16] with a NOESY mixing time of 100 ms and a TOCSY mixing time of 35 ms. All the above experiments employed pulsed field gradients. A 2D NOESY spectrum with a mixing time of 150 ms and a 2D TOCSY spectrum with a mixing time of 80 ms and a 3D TOCSY-NOESY with a NOESY mixing time of 150 ms and a TOCSY mixing time of 50 ms [17] were collected on an unlabelled protein sample at a concentration of 1.3 mM in identical solution conditions except 100% $D_2O$ was used.

Multidimensional Fourier transformation, employing linear prediction, was performed with Varian VNMR version 5.2 software (Varian Associates, Palo Alto, CA). After transformation, the processed data from all experiments except the $^{15}$N-HMQC-J dataset were converted into XEASY format [18] for spectral analysis. All peak picking, spectral analysis and semiautomated resonance assignments were performed with the XEASY software package [18]. $^3J_{HN\alpha}$ coupling constants were estimated from the splittings in the $^{15}$N-HMQC-J dataset by J deconvolution [19] using an 'in house' software package (C.J. Blake and M.A. Keniry, unpublished results).

Hydrogen exchange was performed by lyophilising the $^{15}$N-labelled Long-[Arg-3]-IGF-I solution and reconstituting the sample in 99.9% $D_2O$. A series of $^{15}$N,$^1$H-HSQC spectra was collected at 20°C at intervals of 1 h, 4 h and 24 h. The elapsed time between reconstitution and the start of the first HSQC experiment was 15 min and each HSQC spectrum was acquired in 30 min.

## 3. Results and discussion

### 3.1. Resonance assignment

Spin system identification was achieved by analysis of 2D HSQC-TOCSY and 3D TOCSY-HSQC spectra using well established techniques. Sequential resonance assignment was performed following procedures pioneered by Wüthrich and coworkers [20] and utilised 3D NOESY-HSQC and 3D HSQC-NOESY-HSQC spectra. The proline spin systems were assigned by analysis of 2D NOESY and 3D TOCSY-NOESY spectra. The $^1$H-$^{15}$N sensitivity-enhanced HSQC spectrum of Long-[Arg-3]-IGF-I is presented in Fig. 1. The $^1$H and $^{15}$N resonance assignments have been submitted to the

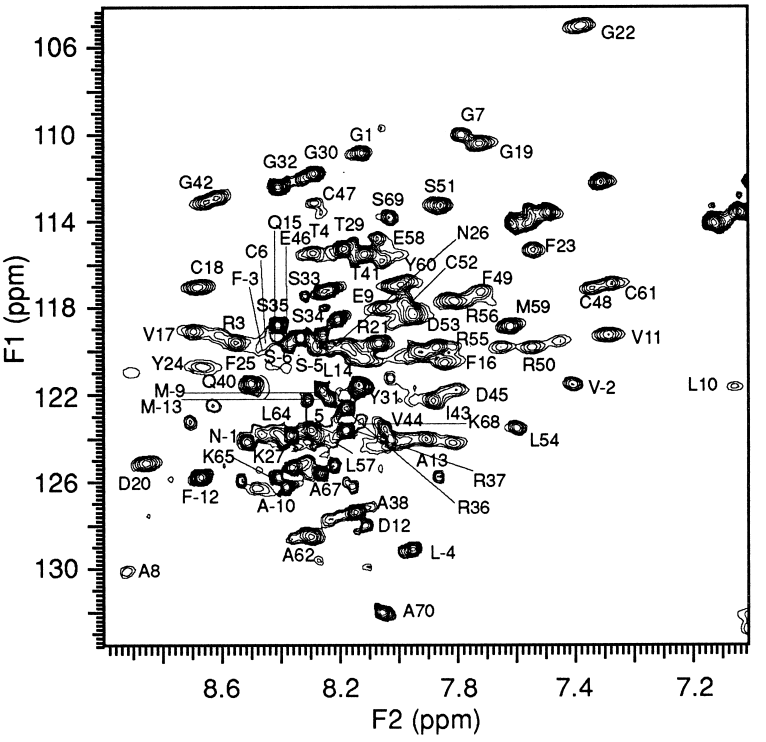


Fig. 1. The $^1$H-$^{15}$N sensitivity enhanced HSQC spectrum of Long-[Arg-3]-IGF-I. Assignments for the backbone amides are labelled.

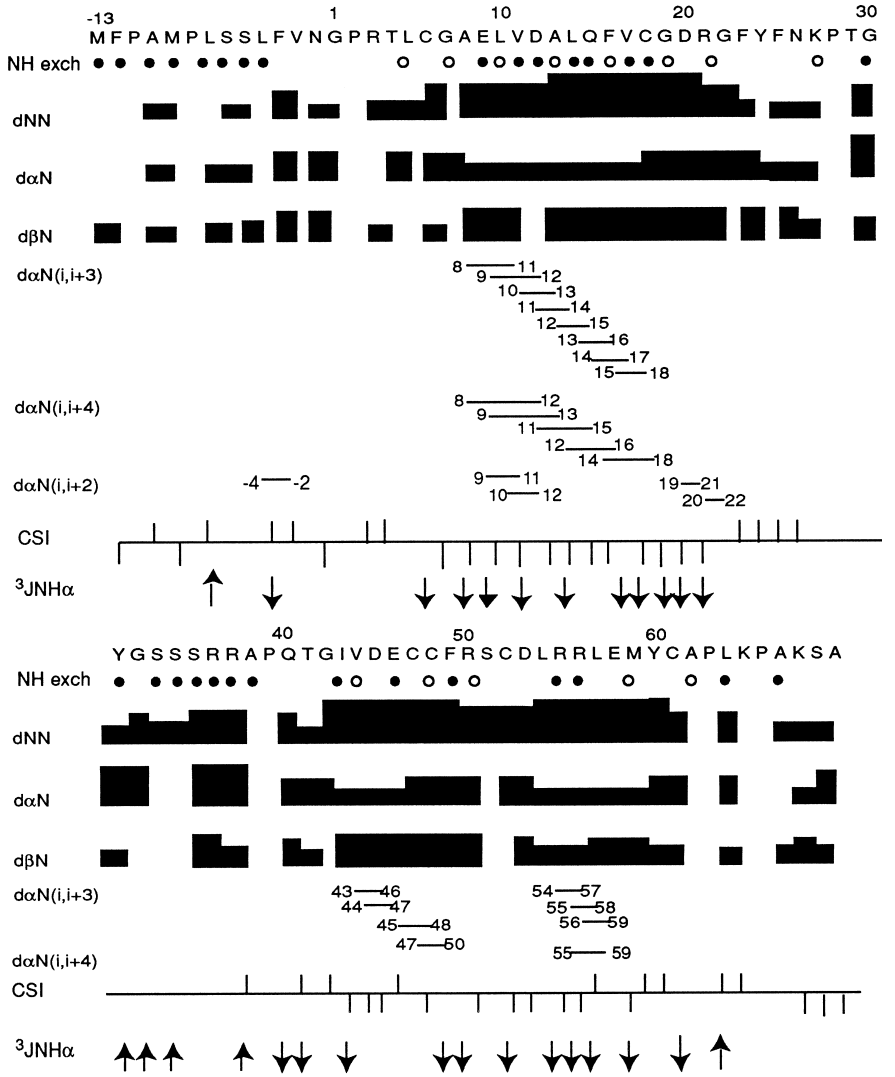


Fig. 2. A summary of the NMR data defining the secondary structure of Long-[Arg-3]-IGF-I at 30°C and pH 4.1. The primary sequence is displayed at the top. Sequential NOE connectivities, $d_{NN}$, $d_{\alpha N}$ and $d_{\beta N}$, are indicated by bars linking the residues concerned and are classified as strong, medium or weak according to the thickness of the bar. Medium range NOE connectivities, $d_{\alpha N}(i,i+2)$, $d_{\alpha N}(i,i+3)$ and $d_{\alpha N}(i,i+4)$, are linked by lines. The chemical shift index (defined as the deviation of the chemical shift value of the α proton from its random coil value by greater than 0.1 ppm) is classified as positive or negative by vertical lines above and below a baseline respectively. $^3J_{HN\alpha}$ values greater than 7.5 Hz are indicated by an upright arrow, $^3J_{HN\alpha}$ values less than 6 Hz are indicated by an inverted arrow. Unfilled circles indicate amide proton resonances that are observable 1 h after exchange of the solvent from $H_2O$ to $D_2O$. Filled circles indicate amide proton resonances that are observed 24 h after solvent exchange.

BioMagResBank (accession number: pending). The amino acid sequence of Long-[Arg-3]-IGF-I is numbered from the N-terminus of the parent human IGF-I. The N-terminus of Long-[Arg-3]-IGF-I is designated as Met-13, the N-terminal extension continues to Asn-1 where the IGF-I domain starts at Gly-1 and proceeds to the C-terminal Ala-70. As well as the 76 major cross-peaks in Fig. 1, there is a subset of low intensity cross-peaks that probably arise from a minor species in solution. None of these low intensity cross-peaks gives rise to observable NOEs in the NOESY-HSQC spectrum. Only one resonance, assigned to Gly-42, is split into two distinct peaks of equal intensity. Inspection of the NOESY-HSQC spectrum revealed an identical NOE pattern for each diagonal peak. Gly-42 is close to Pro-39 and the doubling of its cross-peak may be a result of cis-trans isomerism at this proline.

The secondary structure elements in Long-[Arg-3]-IGF-I were identified from the relative intensities of sequential αN(*i*,*i*+1) and NN(*i*,*i*+1) NOEs, medium range αN(*i*,*i*+2), αN(*i*,*i*+3) and αN(*i*,*i*+4) NOEs, and J coupling information and were confirmed by analysis of the deviation of the chemical shifts of the α-CH protons from their random coil values [21]. A diagrammatic summary of the results of this analysis is presented in Fig. 2.

It is apparent from an examination of the pattern of NOEs of Long-[Arg-3]-IGF-I with the NOEs of the parent protein that the Met-13 to Asn-1 N-terminal extension has very little effect on the secondary structure of the IGF-I domain. Thus, medium to strong sequential NN(*i*,*i*+1) NOEs are observed for the segments Ala-8 to Phe-23, Ile-43 to Arg-50 and Leu-54 to Ala-62 and medium range αN(*i*,*i*+3) NOEs are detected for the segments Ala-8 to Cys-18, Ile-43 to Arg-50 and Leu-54 to Met-59. Furthermore, αN(*i*,*i*+4) NOEs are also observed in these regions (Fig. 2). Such NOE patterns are typically found in the helical regions of proteins and hence this places the

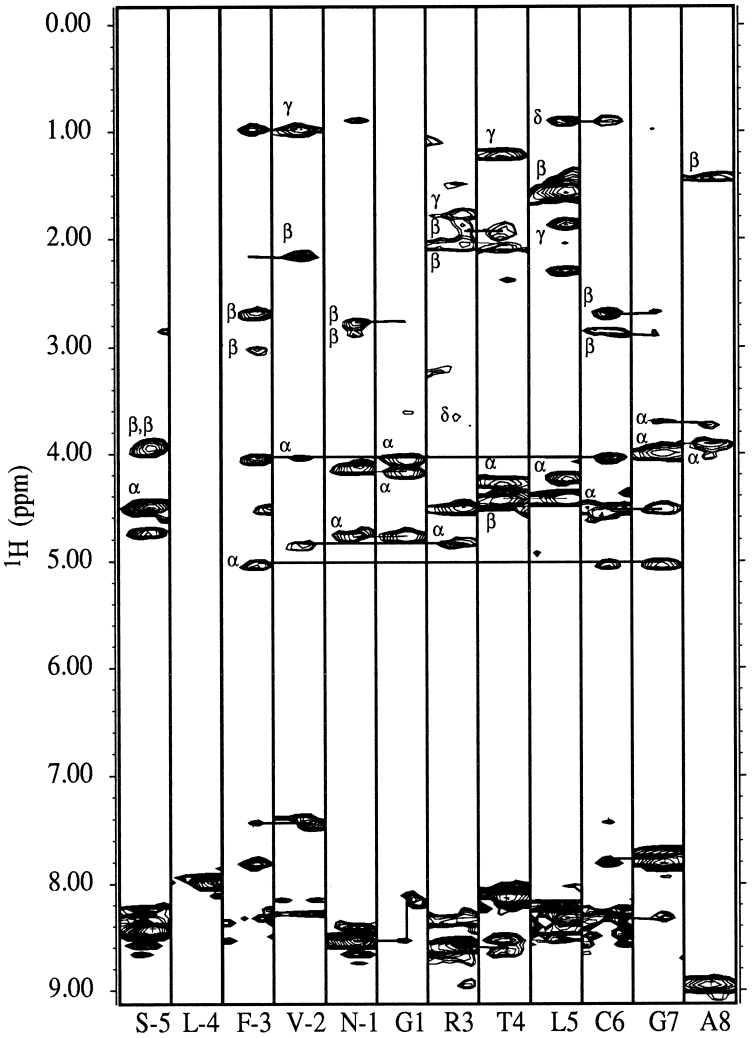


Fig. 3. Strips from the 3D sensitivity enhanced $^{15}$N-NOESY-HSQC spectrum of Long-[Arg-3]-IGF-I displaying the sequential and long range contacts observed for the region from S-5 to L5.

three helices in the IGF-I domain in approximately the same location as in the parent IGF-I protein. Strong αN(*i*,*i*+1) NOEs are observed in the segments Thr-4 to Leu-5, Cys-6 to Ala-8, Gly-19 to Tyr-24 and Thr-29 to Ala-39 suggesting that these regions are in extended conformations as in IGF-I [11–13]. Medium range αN(*i*,*i*+2) NOEs are detected between Gly-19 and Arg-21 and between Asp-20 and Gly-22 indicating that the β-turn observed in this region of IGF-I [11] is preserved in the IGF-I domain of Long-[Arg-3]-IGF-I. The magnitude of some NOEs was uncertain in previous homonuclear studies of IGF-I [11–13] because of overlap in some regions. In this work, these regions are better defined because the pulse sequences employed pulsed field gradients for coherence selection and the resonances were dispersed along the nitrogen dimension of the F2 domain [16]. Rapidly exchanging protons are more readily observed because of these recent technological developments. The Val-11 cross-peak in the HSQC spectrum is broad and shifted upfield as in the native IGF-I [11] suggesting a remarkably similar structural element that is retained at the start of helix 1 near the N-terminal extension. Many of the long range NOEs that are observed in native IGF-I are also observed in the IGF-I domain of Long-[Arg-3]-IGF-I (Fig. 3) suggesting that the addition of the N-terminal extension has little or no effect on the three-dimensional fold of the parent IGF-I domain.

The N-terminal segment of the extension, from Met-13 to Ser-5 has little or no recognisable structure, as judged by the paucity of non-sequential NOEs. Based on the pattern of NOEs, the segment from Leu-4 to Gly-1 has features reminiscent of a turn-type structure. Thus, medium range NOEs are observed between the amide protons of Leu-4 and Val-2 and several 'reversed' sequential NOEs are observed between the amide proton of Phe-3 and the α, β and γ protons of Val-2. On the basis of this NOE pattern it is not possible to assign this turn to any of the standard types. Interestingly, long range NOEs are observed between Phe-3 and Gly-7 and between Val-2 and Cys-6 which place the segment Leu-4 to Gly-1 over the N-terminal end of the IGF-I domain and near the start of helix 1.

Hydrogen-deuterium exchange is frequently used to locate amide protons that are hydrogen-bonded or inaccessible to the solvent. The hydrogen exchange patterns in the IGF-I domain are in agreement with the secondary structure elements and are also consistent with previous homonuclear studies of wild-type IGF-I [11,13]. Helix 1 displays slow amide exchange along the whole length of the helix whereas only

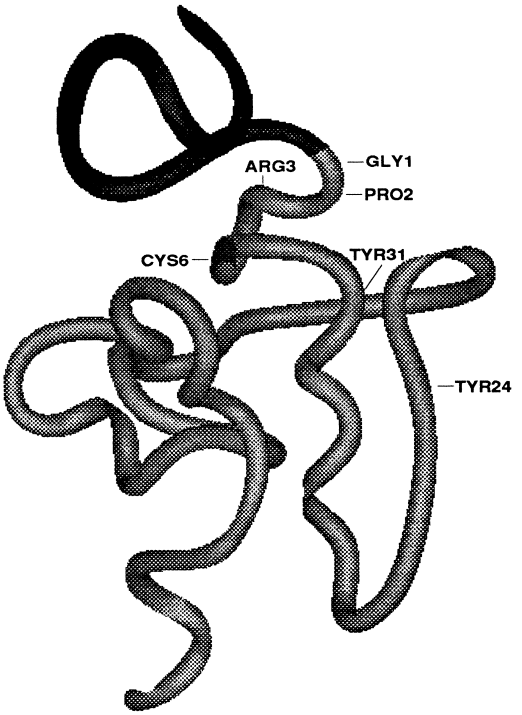


Fig. 4. A diagrammatic representation of the backbone of a preliminary structure of Long-[Arg-3]-IGF-I. The N-terminal extension is shaded dark and the IGF-I domain is shaded light. The location of several residues in the IGF-I domain proximal to the N-terminal extension and Tyr-24 and Tyr-31, which are at the IGF-I receptor binding site, are highlighted.

some of the amide protons within the other two shorter helices are protected from the solvent. Residues within the short stretch of extended structure (Gly-30 to Ala-39) are also protected from solvent. This Gly-30-Ala-39 region of native IGF-I was poorly defined in the homonuclear studies and did not display any solvent protection [11,13], thus it is not clear whether this is a real difference between Long-[Arg-3]-IGF-I and IGF-I or a limitation of the homonuclear studies. IGF-II has a smaller stretch of residues in an extended conformation between helix 1 and helix 2 that are also protected from solvent exchange but, compared to Long-[Arg-3]-IGF-I, this region is offset five residues toward the N-terminus at Gly-25 to Phe-28 [22]. A long stretch of residues in the N-terminal extension (Met-13 to Leu-4) is also protected from solvent. This is a surprising result since most protected amide protons are involved in hydrogen bonds [23] but no well defined secondary structure exists in this part of the N-terminal extension. The pattern of solvent protection may reflect the hydrophobic nature of the extension which arranges the residues in such a way as to exclude solvent but these structures must be transitory since this region is also poorly defined in preliminary distance geometry structural studies.

Previous studies have shown that Glu-3 in the native IGF-I is an important residue in mediating the binding of IGF-I to the IGFBPs [5,7,8]. Thus, removal of the first three N-terminal residues or replacement of Glu-3 with a hydrophobic or a positively charged residue substantially reduces the binding of IGF-I to the IGFBPs [9]. Adding a 13 amino acid hydrophobic N-terminal extension to IGF-I (Long-IGF-I) further reduces the binding to the IGFBPs. Substituting Arg-3 for Glu-3 in Long-IGF-I to form Long-[Arg-3]-IGF-I substantially decreases the binding to the IGFBPs even further. In this variant, the presence of the hydrophobic extension and replacement of Glu-3 with Arg-3 also reduces, to a lesser extent, the binding of the Long-[Arg-3]-IGF-I analogue to the IGF-I receptor compared to native IGF-I but still increases its biological activity five- to ten-fold over the latter [9]. This work has shown that the reduced binding of Long-[Arg-3]-IGF-I to the IGFBPs can be explained in terms of the replacement of Glu-3 by Arg-3 and also by masking the N-terminus of IGF-I from the IGFBPs by the hydrophobic extension. The latter may explain the decreased binding to the IGFBPs and resultant increased biological potency of Long-[Arg-3]-IGF-I compared to native IGF-I. Association of Long-[Arg-3]-IGF-I with the IGFBPs is most likely prevented by steric hindrance caused by the partially structured N-terminal extension impeding access to Gly-1 and Pro-2 combined with the effect of the charge reversal caused by substituting Arg-3 for Glu-3. A preliminary structure of Long-[Arg-3]-IGF-I displaying the proximity of the N-terminal extension (shaded in black) to Gly-1, Pro-2 and Arg-3 and the start of helix 1 is shown in Fig. 4.

An explanation for the reduced binding of Long-[Arg-3]-IGF-I to the IGF-I receptor is less obvious, since the IGF-I receptor recognises mainly aromatic residues at positions 24 and 31 in native IGF-I and to a lesser extent C and A domain residues [24]. Although the start of helix 1 at Ala-8 is a long way from these two aromatic residues in terms of the primary structure, Ala-8 is sufficiently close in space for a point mutation at this residue to reduce the binding of IGF-I to the IGF-I receptor [25]. The observation of long range NOEs between Phe-3 and Val-2 in the extension with Gly-7 and Cys-6 respectively, places the extension sufficiently close to the start of helix 1 to interfere with the binding of Long-[Arg-3]-IGF-I to the IGF-I receptor. It is also possible that there may be non-specific binding of the mobile N-terminal part of the hydrophobic extension of Long-[Arg-3]-IGF-I to the IGF-I receptor thereby preventing the specific binding that is required for the receptor to mediate its biological action.

*Acknowledgements:* The authors would like to acknowledge Prof. K. Wüthrich (ETH, Zürich) for providing us with the XEASY software package and Professor Lewis Kay (University of Toronto, Toronto) for providing us with the code for the sensitivity-enhanced $^{15}N$ pulse sequences. The authors have benefited from the use of NMR facilities at the Australian National University NMR Centre.

## References

[1] Rinderknecht, E. and Humbel, R.E. (1978) J. Biol. Chem. 253, 2769–2776.
[2] Blundell, T.L., Bedarkar, S. and Humbel, R.E. (1983) Fed. Proc. 42, 2542–2547.
[3] Humbel, R.E. (1990) Eur. J. Biochem. 190, 445–462.
[4] Froesch, E.R., Schmid, Chr., Schwandler, J. and Zapf, J. (1985) Annu. Rev. Physiol. 47, 443–467.
[5] Ballard, F.J., Ross, M., Upton, F.M. and Francis, G.L. (1988) Biochem. J. 249, 721–726.
[6] Jones, J.I. and Clemmons, D.R. (1995) Endocr. Rev. 16, 3–34.
[7] Bagley, C.J., May, B.L., Szabo, L., McNamara, P.J., Ross, M., Francis, G.L., Ballard, F.J. and Wallace, J.C. (1989) Biochem. J. 259, 665–671.
[8] King, R., Wells, J.R.E., Krieg, P., Snoswell, M., Brazier, J., Bagley, C.J., Wallace, J.C., Ballard, F.J., Ross, M. and Francis, G.L. (1992) J. Mol. Endocrinol. 8, 29–41.
[9] Francis, G.L., Ross, M., Ballard, F.J., Milner, S.J., Senn, C.,

McNeil, K.A., Wallace, J.C., King, R. and Wells, J.R.E. (1992) J. Mol. Endocrinol. 8, 213–223.
[10] Rinderknecht, E. and Humbel, R.E. (1976) Proc. Natl. Acad. Sci. USA 12, 4379–4381.
[11] Sato, A., Nishimura, S., Ohkubo, T., Kyogoku, Y., Koyama, S., Kobayashi, M., Yasuda, T. and Kobayashi, Y. (1992) J. Biochem. (Tokyo) 111, 529–536.
[12] Cooke, R.M., Harvey, T.S. and Campbell, I.D. (1991) Biochemistry 30, 5484–5491.
[13] Sato, A., Nishimura, S., Ohkubo, T., Kyogoku, Y., Koyama, S., Kobayashi, M., Yasuda, T. and Kobayashi, Y. (1993) Int. J. Pept. Protein Res. 41, 433–440.
[14] Kay, L.E., Keifer, P. and Saarinen, T. (1992) J. Am. Chem. Soc. 114, 10663–10665.
[15] Szyperski, T., Güntert, P., Otting, G. and Wüthrich, K. (1992) J. Magn. Reson. 99, 552–560.
[16] Zhang, O., Kay, L.E., Olivier, J.P. and Forman-Kay, J.D. (1994) J. Biomol. NMR 4, 845–858.
[17] Oschkinat, H., Cieslar, C., Gronenborn, A.M. and Clore, G.M. (1989) J. Magn. Reson. 81, 212–216.
[18] Bartels, C., Xia, T-H., Billeter, M., Güntert, P. and Wüthrich, K. (1995) J. Biomol. NMR 6, 1–10.
[19] Le Parco, J-M., McIntyre, L. and Freeman, R. (1992) J. Magn. Reson. 97, 553–567.
[20] Wüthrich, K. (1986) NMR of Proteins and Nucleic Acids, Wiley, New York.
[21] Wishart, D.S., Bigam, C.G., Holm, A., Hodges, R.S. and Sykes, B.D. (1995) J. Biomol. NMR 5, 67–81.
[22] Torres, A.M., Forbes, B.E., Alpin, S.E., Wallace, J.C., Francis, G.L. and Norton, R.S. (1995) J. Mol. Biol. 248, 385–401.
[23] Englander, S.W. and Kallenbach, N.R. (1984) Q. Rev. Biophys. 16, 521–655.
[24] Cascieri, M.A. and Bayne, M.L. (1989) in: Molecular and Cellular Biology Insulin-like Growth Factors and their Receptors (LeRoith, D. and Raizada, M.K., Eds.), p. 225, Plenum, New York.
[25] Shooter, G.K., Magee, B., Soos, M.A., Francis, G.L., Siddle, K. and Wallace, J.C. (1996) J. Mol. Endocrinol. 17, 237–246.